BIOCHEMISTRY
including biophysical chemistry & molecular biology

Article

pubs.acs.org/biochemistry

Computational Evidence for the Catalytic Mechanism of Tyrosylprotein Sulfotransferases: A Density Functional Theory Investigation

Tainah Dorina Marforio, Pietro Giacinto, Andrea Bottoni,* and Matteo Calvaresi*

Dipartimento di Chimica "G. Ciamician", Alma Mater Studiorum − Università di Bologna, via F. Selmi 2, 40126 Bologna, Italy

Supporting Information

ABSTRACT: In this paper we have examined the mechanism of tyrosine *O*-sulfonation catalyzed by human TPST-2. Our computations, in agreement with Teramoto's hypothesis, indicate a concerted S_N2-like reaction (with an activation barrier of 18.2 kcal mol^{-1}) where the tyrosine oxygen is deprotonated by Glu^{99} (base catalyst) and simultaneously attacks as a nucleophile the sulfuryl group. For the first time, using a quantum mechanics protocol of alanine scanning, we identified unequivocally the role of the amino acids involved in the catalysis. Arg^{78} acts as a shuttle that "assists" the sulfuryl group moving from the 3′-phosphoadenosine-5′-phosphosulfate molecule to threonine and stabilizes the transition state (TS) by electrostatic interactions. The residue Lys^{158} keeps close the residues participating in the overall H-bond network, while Ser^{285}, Thr^{81}, and Thr^{82} stabilize the TS via strong hydrogen interactions and contribute to lower the activation barrier.

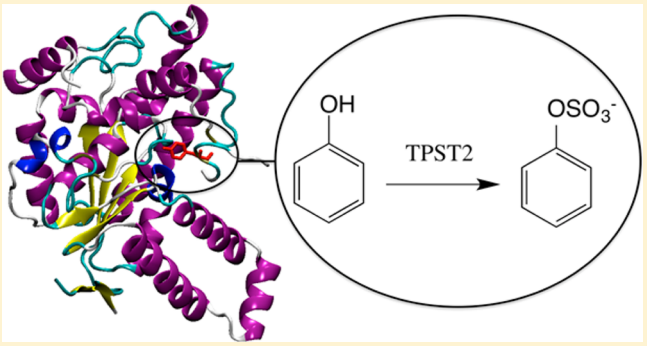

Sulfonation of biomolecules in prokaryotes and multicellular species is a metabolic route of primary importance. Enzymes involved in this metabolic process are sulfotransferases (ST) that catalyze the transfer of a sulfuryl group $SO_3^{(-)}$ from an activated donor to a substrate containing hydroxyl groups or amino groups acting as nucleophiles.[1] There are two vast classes of STs: cytosolic and membrane-associated sulfotransferases. The first ones are involved in hormone regulation, drug metabolism, and detoxification, while the membrane-associated sulfotransferases are responsible for the sulfonation of carbohydrates and proteins. Also, they are known to play a key role in the biochemical signaling pathway and molecular recognition. The first studies on STs focused on cytosolic proteins.[2] More recently membrane-associated STs were carefully examined demonstrating their central role in biological processes.[3]

Tyrosine *O*-sulfonation was first observed in 1954 by Bettelheim in bovine fibrinopeptide B^4 and was considered to be very rare and confined to fibrogen and a few other proteins until 1982, when Huttner demonstrated that all tissues in rats contain proteins with *O*-sulfated tyrosine residues.[5] Tyrosine sulfonation was afterward observed in many mammalian tissues and cells, and in the mid-1980 this reaction was demonstrated to be catalyzed by tyrosylprotein sulfotransferase[6] (EC 2.8.2.20), a membrane-associated protein situated in the *trans*-Golgi network.[7] The interest in tyrosine *O*-sulfonated peptides increased in the second half of the 1990s, when Farzan reported that chemokine receptor CCR5 (a G-protein coupled receptor belonging to the cytokine receptor class, important in cell signaling) behaves as a coreceptor for immunodeficiency viruses (HIV) and is tyrosine *O*-sulfonated.[8] Furthermore, at the beginning of the 21st century, tyrosine sulfonation was shown to be involved in inflammation processes, such as asthma and chronic pulmonary diseases.[9] Also, sulfonation of tyrosine residues was revealed to be critical in atherosclerosis progression.[10]

Tyrosylprotein sulfotransferases (TPSTs) are a particular group of membrane sulfotransferases that transfer a sulfuryl group from the cofactor 3′-phosphoadenosine-5′-phosphosulfate molecule (PAPS) to the hydroxyl group of a protein-bound tyrosine to form a *O*-sulfated tyrosine and 3′-phosphoadenosine-5′-phosfate (PAP) (see Figure 1). A significant advance in understanding TPST operating principles was made possible by the molecular cloning in 1998 of two TPST isoforms (TPST-1 and TPST-2)[11,12] from mouse and human. TPST-1 and TPST-2, which are probably coexpressed in all mammalian cells, have a similar size, consisting of a sequence of 370 and 377 amino acids, respectively, and sharing 64% amino acid sequence identity. Each TPST gene encodes a protein with a short eight-residue cytosolic region that contains the *N*-terminus of the protein, a single ∼17 residue transmembrane region (TM), a putative ∼40 residue stem region, and a catalytic region that is located on the luminal side of the membrane. Since no X-ray diffraction data were available until 2013, information on

Received: April 1, 2015
Revised: June 17, 2015
Published: June 25, 2015

DOI: 10.1021/acs.biochem.5b00343
Biochemistry 2015, 54, 4404−4410

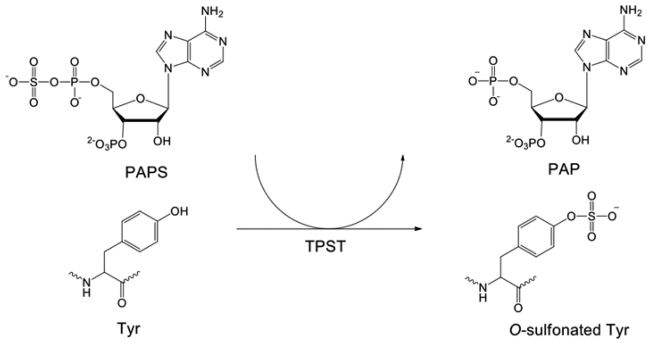

Figure 1. A schematic representation of the TPST catalyzed tyrosine *O*-sulfonation reaction.

TPSTs were based on sequence comparison with other STs of known structure. Further information was obtained from mass spectroscopy, sulfonation inhibition, metabolic labeling, and amino acid analysis.[13] Only very recently, after crystallization of the human TPST-2, have the X-ray diffraction data become available.[14] The crystallization of the core domain of human TPST-2 (Gly^{43}-Leu^{359}), usually denoted as TPST2ΔC18, has proven that TPST-2 is a homodimer consisting of two protomers, denoted as protomer A and protomer B. The existence of TPST-2 as a dimer has been further supported by gel filtration chromatography: in that experiment TPST2ΔC18 was eluted with a mass of 77 kDa, a result consistent with the dimeric structure.[14] Among the three different crystal structures of TPST-2 deposited in the Protein Data Bank,[14] in the present study we have used that denoted as 3AP1, which shows the best resolution (1.9 Å). This structure includes the cofactor after loss of the sulfuryl group (PAP) and the substrate C4P5Y3, a peptide derived from complement component C4, a blood protein involved in the complement system, which constitutes a part of the immune system. At the beginning of 1990 it was demonstrated that complement C4 binds TPST-2 and that tyrosine *O*-sulfonation involves the sequence Glu−Asp−Tyr−Glu−Asp−Tyr−Glu−Tyr−Asp−Glu, which has three suitable sulfonation sites.[15,16] The peptidic sequence chosen by Teramoto for the crystallization of the TPST-2 system was a region of nine amino acids based on human complement C4 and including only one sulfonation site. This peptide, named C4P5Y3, has the sequence Asp−Phe−Glu−Tyr^{1006}−Asp−Glu−Phe−Asp−Glu where Tyr^{1006} is the sulfonation site. Even if there is no consensus yet on the mechanism of tyrosine *O*-sulfonation, during the few last years two hypotheses have been proposed. In 2010, on the basis of mass spectroscopy and kinetics analysis, Danan proposed a *ping-pong* mechanism,[17] in which a histidine residue behaves as a sulfuryl group carrier. More recently Teramoto has suggested an alternative mechanistic hypothesis (S_N2-like mechanism) where Arg^{78} and Glu^{99} act as a acatalytic acid and base, respectively. Moreover, he hypothesized that Lys^{158} and Ser^{285} residues play a key role in stabilizing the transition state. A schematic representation of Teramoto's mechanism is given in Figure 2.

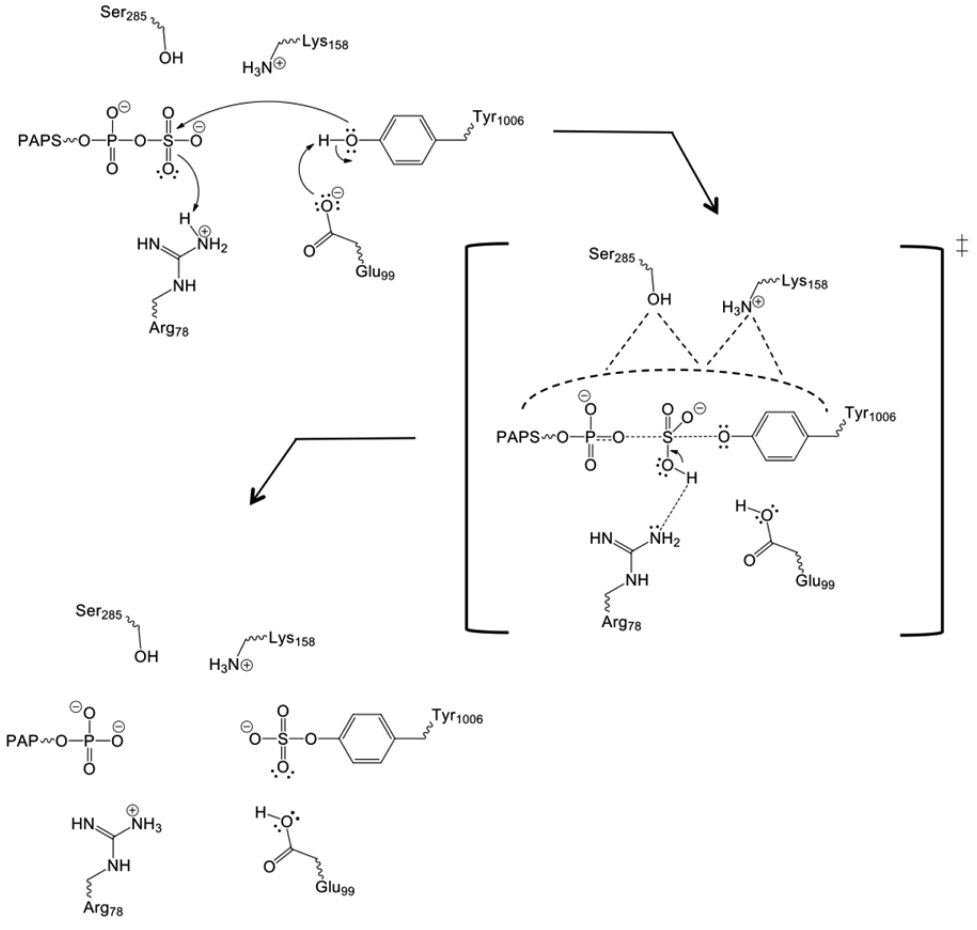

Figure 2. A schematic representation of Teramoto's mechanistic hypothesis.

DOI: 10.1021/acs.biochem.5b00343
Biochemistry 2015, 54, 4404−4410

While the recognition/binding of human TPST-2 has been recently investigated,[18] as far as we know to date no studies are available to clarify its catalytic mechanism. Since the knowledge of the crystal structure of this enzyme makes it now possible to build reliable model-systems, in the present paper we carry out a detailed density functional theory (DFT) computational investigation of the mechanism of tyrosine *O*-sulfonation catalyzed by the human TPST-2 enzyme. This methodology has been shown to be successful to study enzymatic mechanisms.[19−23] Our goal is to outline the mechanistic scheme of the TPST-2 catalyzed reaction to understand the role of various residues in the catalysis and the possible involvement of an histidine residue as a sulfuryl group carrier.

COMPUTATIONAL DETAILS

Choice of the Quantum-Mechanical Model-System. To model the active site of human TPST-2 we used the X-ray crystal structure *3AP1* (TPST2ΔC18, C4 peptide and PAP),[14] to which we added manually the sulfuryl group $SO_3^{(-)}$. The hydrogen atoms were included in the *3AP1* structure at pH 7.4 using the H++ online program.[24]

The choice of a suitable model-system is crucial in the investigation of an enzyme mechanism, and it must primarily include all groups that are supposed to play a key role in the reaction. Thus, to examine in detail the S_N2-like mechanism proposed by Teramoto,[5] starting from the X-ray crystal structure *3AP1*, we built a model-system including Glu^{99} and Arg^{78} that are postulated to behave as a catalytic base and acid, respectively. Also, we added Ser^{285} and Lys^{158} that are supposed to stabilize the transition state. Furthermore, we considered initially all long-range interactions between TPST2ΔC18, C4P5Y3, and PAPS. Then, to reduce the size of the resulting model-system we cut off the residues farther than 8 Å from the sulfonation site, i.e., the hydroxylic oxygen (O^{193}) of the Tyr^{1006} side-chain. Finally, to reduce further the number of atoms, we discarded those parts of PAPS and C4P5Y3 that were not directly involved in the reaction, i.e., the adenine ring and the 3′-phosphate of PAPS and all residues of C4P5Y3 except Tyr^{1006}. The cut bonds were replaced by bonds with hydrogen atoms. In summary, in addition to Tyr^{1006} and the cut PAPS, our model-system includes (a) the four critical residues Glu^{99}, Arg^{78}, Ser^{285}, Lys^{158}; (b) Pro^{77}, Thr^{81}, Thr^{82} that interact specifically with Tyr^{1006} and the 5′PS group of PAPS; (c) Val^{76}, Ile^{199}, Asp^{159}, Phe^{161}, Pro^{160}, Val^{197}, Gly^{80}, and Asp^{159} which surround the reaction site. The size of all these residues was reduced by an appropriate cut of conveniently chosen chemical bonds (in particular, the bonds involving the α carbons). The cut bonds were again replaced by bonds with hydrogen atoms. The resulting model-system finally used in DFT computations is schematically represented in Figure S1. It involves 241 atoms and the total charge is −1.

QM Calculations. All reported DFT computations were carried out with the Gaussian 09 series of programs[25] on the model-system obtained from the crystal structure. The M06-2X functional was employed.[26] The geometries of the various critical points on the potential surface were optimized with the gradient method available in Gaussian 09, and harmonic vibrational frequencies were computed to evaluate the nature of all critical points. The system was partitioned into two regions, which were assigned basis sets of different accuracy. The atoms of one region were those directly involved in the reaction (i.e., Tyr^{1006} side-chain, Glu^{99} side-chain, and 5′-phosphosulfate moiety) or in the formation of hydrogen bonds with the reacting core (i.e., Lys^{158} side-chain): for these atoms we used the 6-31+G* basis set.[25] The other region included all remaining atoms which were described by the 3-21G* basis set.[25] The level of accuracy used for the various atoms are schematically indicated in Figure S2. This basis set (denoted as 6-31+g*/3-21g*) corresponds to a total of 1462 basis functions. ZPE corrections were taken into account. In our experience this approach can provide an accurate description of enzymatic reactions at a reasonable computational cost.[27−29] However, to check the accuracy of this basis we carried out single point computations on the optimized geometries with the TZVP basis set[25] (corresponding to a total of 2858 basis functions). Furthermore, we considered ZPE corrections obtained at the lower level of accuracy.

Emulating the Protein Environment. To emulate the partially constraining effect of the protein environment, during the geometry optimization process we kept "frozen" to their crystallographic coordinates the positions of appropriately chosen atoms: these were mainly the hydrogens added in place of the cut bonds and the atoms near the border of the model-system and not directly involved in the reaction or in hydrogen bond formation. This approach preserves the geometry of the active-site cavity and avoids the possibility that the TPST-2 active site secondary structure will run into unwanted conformational changes. The "frozen" atoms are marked by contour lines in Figure S1. Furthermore, the effect of the entire protein environment was evaluated with the polarizable continuum model (PCM),[30] as implemented in Gaussian 09. We used a value of 4.24 (corresponding to diethyl ether) for the dielectric constant ε.[31] This value is close to 4.0, which is the value generally chosen to describe the surrounding protein and to account for the simultaneous presence of hydrophilic and hydrophobic groups around the active site.[32]

RESULTS AND DISCUSSION

Danan Mechanism. In the ping-pong[17] mechanism proposed by Danan, the His^{91} residue is assumed to act as a carrier for the sulfuryl group; to check the reliability of this hypothesis we evaluated the distance between His^{91} (τ nitrogen) and the sulfuryl group (S^{212}) of PAPS in the 3AP1 structure. We found a value of 22.7 Å, which is evidently too large to allow the histidine residue to clasp the $SO_3^{(-)}$ group. Moreover, to evaluate the possibility that other histidine residues in the vicinity of the active site could be involved as a possible carrier, we examined in various cases the distance between the histidine τ nitrogen[6] and the S^{212} atom of the 5′PS moiety of PAPS. These distances are in all cases very large (in the range 8−22.5 Å) suggesting that none of the examined histidine residues are in a suitable position to behave as a sulfuryl carrier. These values are reported in Table 1. A 80 ns molecular dynamics (MD) confirms that the above-mentioned histidine residues do not significantly move from their initial

Table 1. Distance Values (Ångstroms) between the S^{212} Atom of the 5′PS Moiety of PAPS and the τ Nitrogen of Various Histidine Residues[a]

histidine residue	His^{91}	His^{148}	His^{190}	His^{244}	His^{266}	His^{267}	His^{304}
distance S^{212}−τ nitrogen atom	20.2	22.5	13.6	17.3	16.5	7.9	18.4

[a]This value is obtained as average value along the 80 ns MD simulation.

DOI: 10.1021/acs.biochem.5b00343
Biochemistry 2015, 54, 4404−4410

positions, which allows us to definitely discard Danan's hypothesis (MD computational details are reported in Supporting Information; MD computations were exclusively carried out to check Danan's hypothesis).

Teramoto Mechanism. The mechanism of the sulfuryl group transfer in human TPST-2 involves the PAPS cofactor which donates the sulfuryl group to the hydroxyl group of tyrosine (Tyr^{1006}) in the substrate C4P5Y3. The products are the *O*-sulforylated tyrosine and PAP. The computed energy profile (at the DFT level) indicates that the reaction proceeds through a concerted mechanism. The corresponding critical points are the starting enzyme−substrate complex (ES), the transition state (TS) and the final enzyme−product complex (EP). A schematic representation of the three critical points, including only the closest atoms around PAPS, is given in Figures 3−5. The computations carried out at the 6-31+g*/3-21g* level show that an activation barrier of 18.5 kcal mol^{-1} must be surmounted to reach EP, which is 5.7 kcal mol^{-1} above the starting complex. These values do not change significantly at the TZVP level: they become 20.8 and 7.7 kcal mol^{-1}, respectively, suggesting that the 6-31+g*/3-21g* basis is a reliable level of accuracy to describe the model-system. It is reasonable to believe that the difference found between the two accuracy levels could be further reduced after geometry optimization.

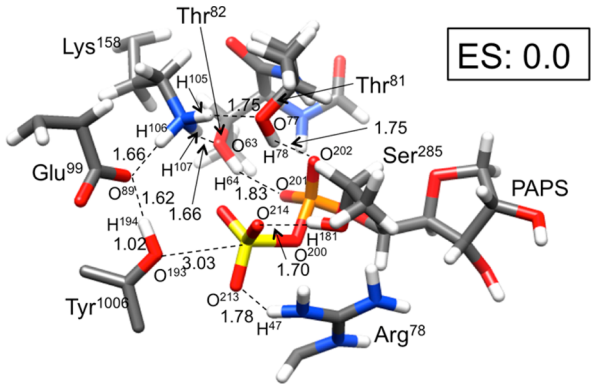

Figure 3. A partial schematic representation (including only the closest atoms around PAPS; see Supporting Information for the full model) of the starting enzyme−substrate complex ES. The reported energy value (kcal mol^{-1}) is relative to ES. Bond lengths are in Å.

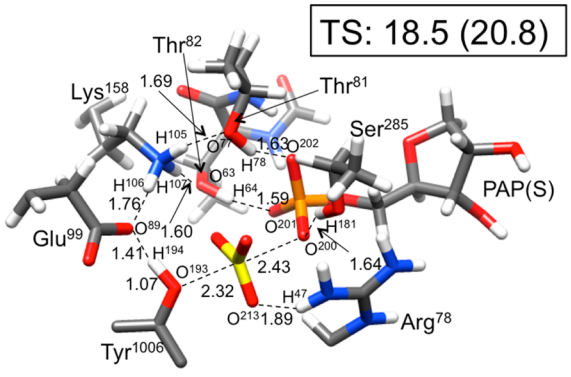

Figure 4. A partial schematic representation (including only the closest atoms around PAPS; see Supporting Information for the full model) of the transition state TS. The reported energy value (kcal mol^{-1}) is relative to ES (in parentheses the value obtained with the TZVP basis set). Bond lengths are in Å.

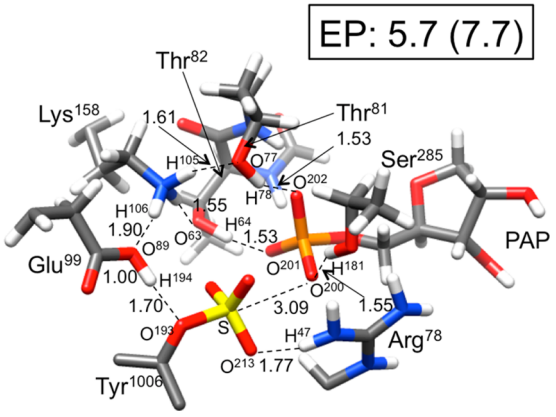

Figure 5. A partial schematic representation (including only the closest atoms around PAPS; see Supporting Information for the full model) of the final enzyme−product complex EP. The reported energy value (kcal mol^{-1}) is relative to ES (in parentheses the value obtained with the TZVP basis set). Bond lengths are in Å.

The hydrogen transfer between the Tyr^{1006} hydroxyl group to the Glu^{99} carboxylate group (H^{194} moving from O^{193} to O^{89}) is crucial in the reaction scheme proposed by Teramoto because it generates the nucleophilic oxygen (O^{193} belonging to Tyr^{1006}) that attacks the sulfuryl group. Interestingly, in the ES starting complex H^{194} already forms a strong hydrogen bond with O^{89} ($H^{194\cdots}O^{89}$ distance is 1.62 Å). This interaction anticipates the subsequent proton transfer that activates O^{193} as a nucleophile.

Lys^{158} and Ser^{285}, which are hypothesized to stabilize the transition state in the Teramoto's reaction scheme, are involved in rather important interactions. In particular the three hydrogen atoms of the protonated Lys^{158} form strong hydrogen bonds with Glu^{99}, Thr^{81}, and Thr^{82}: the $H^{106}\cdots O^{89}(Glu^{99})$, $H^{105}\cdots O^{77}(Thr^{81})$ and $H^{107}\cdots O^{63}(Thr^{82})$ distances are 1.66, 1.75, and 1.66 Å, respectively. Similarly, the hydroxyl hydrogen of Ser^{285} strongly interacts with the SO_3 group bonded to PAPS (the $H^{181}(Ser^{285})\cdots O^{214}(SO_3)$ distance is 1.70 Å). Additional significant interactions help to maintain atoms in the ES complex in a suitable position for reactions. These are (i) interaction between Arg^{78} and the sulfuryl group of PAPS ($H^{47}(Arg^{78})\cdots O^{213}$ = 1.78 Å); (ii) interaction between Thr^{81} hydroxyl group and the 5′-phosphate of PAPS ($H^{78}\cdots O^{202}$ = 1.75 Å); (iii) a similar interaction involving Thr^{82} and the 5′-phosphate group ($H^{64}\cdots O^{201}$ = 1.83 Å).

In the transition state (characterized by an imaginary frequency of 214,748 cm^{-1}) a planar sulfuryl moiety is moving from O^{200} to O^{193}. The $SO_3^{(-)}$ group is approximately halfway between the two oxygen atoms, the $O^{193}\cdots S^{212}$ and $O^{200}\cdots S^{212}$ distances being 2.32 and 2.44 Å, respectively. The TS structure clearly shows that Glu^{99} behaves as a base catalyst, as suggested by Teramoto: H^{194} is now closer to $O^{89}(Glu^{99})$ ($H^{194}\cdots O^{89}$ distance is 1.41 Å) with a consequent weakening of the O^{193}–H^{194} bond (from 1.02 Å in ES to 1.07 Å in TS). Thus, TS is a concerted highly asynchronous transition state where the approach of SO_3 to tyrosine oxygen triggers the tyrosine deprotonation. This is confirmed by the shape of the transition vector obtained in the frequency computation. Interestingly, $SO_3^{(-)}$ remains anchored to Arg^{78} by means of the strong interaction with the sulfuryl oxygen O^{213} (the $H^{47}\cdots O^{213}$ distance is 1.89 Å) suggesting that the arginine residue does not behave as an acid catalyst by donating a proton to the

DOI: 10.1021/acs.biochem.5b00343
Biochemistry 2015, 54, 4404−4410

Table 2. Activation Barrier E_a (kcal mol^{-1}) Computed after Replacement of Each Residue Reported on the Left Column with Alanine[a]

mutated residue	interaction	activation barrier E_a	ΔE_a	Mulliken charge on SO_3
Arg^{78}	salt bridge involving $SO_3^{(-)}$	22.3	4.1	ES: −0.58
				TS: −0.38
Lys^{158}	$H^{105}\cdots O^{77}$, $H^{106}\cdots O^{89}$, and $H^{107}\cdots O^{63}$ H-bonds	18.8	0.6	ES: −0.47
				TS: −0.43
Ser^{285}	$H^{181}\cdots O^{200}(SO_3)$ and $H^{181}\cdots O^{202}$(PAPS) H-bonds	22.9	4.7	ES: −0.72
				TS: −0.55
Thr^{81}	$H^{78}\cdots O^{202}$ (PAPS) H-bonds	22.7	4.0	ES: −0.43
				TS: −0.36
Thr^{82}	$H^{64}\cdots O^{201}$ (PAPS) H-bonds	23.7	5.5	ES: −0.51
				TS: −0.40

[a]For each residue a short description of the main interactions is reported. ΔE_a (kcal mol^{-1}) is the variation with respect to the non-mutated enzyme (18.2 kcal mol^{-1}). For each mutated form the net SO_3 Mulliken charges in ES and TS are reported.

migrating sulfuryl group (as hypothesized in Teramoto's scheme) but acts as a shuttle for $SO_3^{(-)}$ following its "travel" along the reaction path. The interactions involving Lys^{158} and the two residues Thr^{81} and Thr^{82} become more important in the TS as suggested by the decrease of the two distances $H^{105}\cdots O^{77}(Thr^{81})$ and $H^{107}\cdots O^{63}(Thr^{82})$ (1.69 and 1.60 Å, respectively). Furthermore, a strong stabilizing interaction (made possible by the transfer of the $SO_3^{(-)}$ group) is established between the hydroxyl hydrogen of Ser^{285} and the oxygen O^{200} of PAPS, which is losing the sulfuryl group ($H^{181}(Ser^{285})\cdots O^{200}$(PAPS) distance is 1.64 Å). A significant increase of the stabilizing effect is also observed for the interaction between the Thr^{81} hydroxyl group and the 5′-phosphate of PAPS (the $H^{78}(Thr^{81})\cdots O^{202}$(PAPS) distance varies from 1.75 Å in ES to 1.63 Å in TS). A further stabilization of TS is provided by the interaction of Thr^{82} with the 5′-phosphate of PAPS. In this case the $H^{64}(Thr^{82})\cdots O^{201}$(PAPS) distance varies from 1.83 Å in ES to 1.59 Å in TS.

Furthermore, we examined the possibility of an alternative mechanism where the proton transfer (from O^{193} to O^{89}) and the attack of the tyrosine oxygen O^{193} on the SO_3 group occur in two separate kinetic steps. In spite of an extensive search we could not locate any intermediate corresponding to deprotonated tyrosine, and we discarded the possibility of a two-step nonconcerted mechanism.

In the final complex EP the sulfuryl group is definitively bonded to the tyrosine residue Tyr^{1006}, and the hydrogen H^{194} has been completely transferred to Glu^{99} (O^{89}−H^{194} distance is 1.00 Å). A strong hydrogen bond involving O^{193} of tyrosine persists, the $O^{193}\cdots H^{194}$ distance being 1.70 Å. Furthermore, the SO_3 group is still anchored to Arg^{78} ($H^{47}\cdots O^{213}$ distance = 1.77 Å), which confirms the role played by the arginine residue in "accompanying" the sulfuryl group (shuttle) along the reaction pathway. On the whole the remaining part of the structure does not significantly differ from that of the ES complex. The most important exception are represented by (a) the hydrogen bond between the serine hydroxyl hydrogen (H^{181}) and O^{200} ($H^{181\cdots}O^{200}$ distance = 1.55 Å) and (b) the two hydrogen bonds involving Thr^{81} ($H^{78}\cdots O^{202}$) and Thr^{82} ($H^{64}\cdots O^{201}$) that become stronger in EP, the corresponding distances being 1.53 Å in both cases (1.75 and 1.83 Å in ES, respectively). These three hydrogen interactions certainly contribute to stabilize the product complex, which remains nevertheless 5.7 kcal mol^{-1} above ES.

A Virtual Mutagenesis Experiment. To quantify the catalytic effect of the residues playing a key role in the sulfuryl exchange reaction (Lys^{158} and Ser^{285}, as suggested by Teramoto, Arg^{78}, Thr^{81}, and Thr^{82}), we carried out a virtual mutagenesis experiment by alanine scanning: thus, we replaced each of these residues with alanine, and we recomputed the energy barrier (fingerprint analysis)[33−35] at the 6-31+g*/3-21g* level. In these computations we neglected the ZPE corrections, but we included the solvent effects. Thus, these barriers must be compared with the value of 18.2 kcal mol^{-1}, which is the barrier obtained for the nonmutated enzyme without ZPE corrections.

The results (collected in Table 2) clearly demonstrate the stabilizing effects exerted by the various residues. The effect on the barrier is significant in all cases (in the range 4.0−5.5 kcal mol^{-1}) except for Lys^{158}: for this residue the increase is only 0.6 kcal mol^{-1} and can be ascribed to the trend of the three H-bonds involving Lys^{158} ($H^{105}\cdots O^{77}$, $H^{106}\cdots O^{89}$ and $H^{107}\cdots O^{63}$) that do not change significantly on passing from ES to TS. We can conclude that Lys^{158}, even if not interacting with the groups directly involved in the reaction, plays an important role in keeping close the residues participating to the overall H-bond network that stabilizes TS. In particular, the above analysis confirms that the stabilization of TS (and the consequent decrease of the activation barrier) via strong hydrogen interactions can be ascribed to Ser^{285} (as suggested by Teramoto) and to other residues such as Thr^{81} and Thr^{82}. These residues exert in ES a sort of "kicking effect" on the sulfuryl group, since they facilitate its detachment by stabilizing the incipient negative charge on the phosphate group of PAPS. The stabilizing effect on TS of Arg^{78} (that anchors $SO_3^{(-)}$ along the whole reaction path and acts as a shuttle following the sulfuryl "travel") is due to a salt bridge, dominated by electrostatic interactions between the negative charge of sulfuryl and the positive charge of arginine.

To obtain a more complete picture of the stabilizing effect of the various residues we have estimated the total charge of the SO_3 group in the reactant complex ES and transition state TS for the nonmutated enzyme and each mutated forms of Table 2. In the nonmutated enzyme the net SO_3 charge is −0.98 in ES and −0.50 in TS: this significant decrease of the charge is further evidence for the stabilizing effect of the various interactions that delocalize the SO_3 charge on passing from reactants to transition state. Interestingly, the charge variation is much less significant when the various residues are replaced by alanine and the corresponding delocalizing interactions partly disappear.

DOI: 10.1021/acs.biochem.5b00343
Biochemistry 2015, 54, 4404−4410

CONCLUSIONS

In this paper we have examined the mechanism of tyrosine *O*-sulfonation catalyzed by human TPST-2. Our DFT computations have confirmed in outline Teramato's general scheme, i.e., a concerted highly asynchronous S_N2-like reaction (with an activation barrier of 18.5 kcal mol^{-1}) where the tyrosine oxygen is deprotoned by Glu^{99} (that acts as a base catalyst as suggested by Teramoto) and simultaneously attacks as a nucleophile the sulfuryl group. Arg^{78} plays a different role from that proposed by Teramoto (acid catalyst). A strong hydrogen interaction involving the sulfuryl oxygen and Arg^{78} allows this group to anchor $SO_3^{(-)}$ along the whole reaction path, acting as a shuttle that follows the sulfuryl "travel" from PAPS to threonine.

After a careful analysis of the structural features of the reactant-complex (ES) and TS and using a QM protocol of "alanine scanning", we could identify unequivocally the role of the amino acids involved in the catalysis. In addition to the "assistance" of Arg^{78} toward the sulfuryl group moving from PAPS to threonine, we found that (i) the stabilizing effect of Arg^{78} on TS is due to a salt bridge, dominated by electrostatic interactions between the negative charge of sulfuryl and the positive charge of arginine; (ii) Ser^{285}, Thr^{81}, and Thr^{82} stabilize TS via strong hydrogen interactions (in particular, these three residues exert a sort of "kicking effect" in the starting reactant-complex, since they facilitate the detachment of sulfuryl group by stabilizing the incipient negative charge on the phosphate group of PAPS); (iii) the role of Lys^{158} is that of keeping close the residues participating to the overall H-bond network that stabilizes TS.

A careful analysis of the structure of enzyme and MD simulations helped us to exclude the Danan's ping-pong mechanism where the His^{91} residue is proposed to act as a carrier for the sulfuryl group. This group and His^{91} are too far away to make possible a mutual significant interaction. Similarly, too large distances have been evidenced for other histidine residues around $SO_3^{(-)}$ that in principle could act as a carrier. However, we cannot exclude, in principle, the possibility of secondary reaction channels leading to the formation of covalent intermediates congruent with Danan's experimental evidence and where another residue replaces the histidine residue suggested by Danan.

We believe that all these results can be extremely useful in the design of mutated forms of the enzyme and in the synthesis of possible antagonists to enhance or decrease the tyrosine *O*-sulfonation of the target substrate.

ASSOCIATED CONTENT

Supporting Information

Representation of the full model-system used in our computations. Atoms kept "frozen" during geometry optimization (Figure S1) and basis set assignment (Figure S2). Molecular dynamics (MD) protocol. Cartesian coordinates (Ångstroms) and total energy values (hartree) for the starting enzyme−substrate complex ES, transition state TS, and final enzyme−product complex EP computed at the M06-2X level. The Supporting Information is available free of charge on the ACS Publications website at DOI: 10.1021/acs.biochem.5b00343.

AUTHOR INFORMATION

Corresponding Authors

*(A.B.) E-mail: andrea.bottoni@unibo.it.

*(M.C.) E mail: matteo.calvaresi3@unibo.it.

Notes

The authors declare no competing financial interest.

REFERENCES

(1) Chapman, E., Best, M. D., Hanson, S. R., and Wong, C. H. (2004) Sulfotransferases: structure, mechanism, biological activity, inhibition, and synthetic utility. *Angew. Chem., Int. Ed. 43*, 3526−3548.

(2) Kakuta, Y., Pedersen, L. G., Carter, C. W., Negishi, M., and Pedersen, L. C. (1997) Crystal structure of estrogen sulphotransferase. *Nat. Struct. Biol. 4*, 904−908.

(3) Moore, K. L. (2003) The Biology and Enzymology of Protein Tyrosine O-Sulfation. *J. Biol. Chem. 278*, 24242−24246.

(4) Bettelheim, F. R. (1954) Tyrosine-O-sulfate in a peptide from fibrinogen. *J. Am. Chem. Soc. 76*, 2838−2839.

(5) Huttner, W. B. (1982) Sulphation of tyrosine residues - a widespread modification of proteins. *Nature 299*, 273−276.

(6) Lee, R. W., and Huttner, W. B. (1985) (Glu62, Ala30, Tyr8)n serves as high-affinity substrate for tyrosylprotein sulfotransferase: a Golgi enzyme. *Proc. Natl. Acad. Sci. U. S. A. 82*, 6143−6147.

(7) Niehrs, C., and Huttner, W. B. (1990) Purification and characterization of tyrosylprotein sulfotransferase. *EMBO J. 9*, 35−42.

(8) Farzan, M., Mirzabekov, T., Kolchinsky, P., Wyatt, R., Cayabyab, M., Gerard, N. P., Gerard, C., Sodrosky, J., and Choe, H. (1999) Tyrosine sulfation of the amino terminus of CCR5 facilitates HIV-1 entry. *Cell 96*, 667−676.

(9) Liu, J., Louie, S., Hsu, W., Yu, K. M., Hugh, B. N., Jr., and Rosenquist, G. L. (2008) Tyrosine sulfation is prevalent in human chemokine receptors important in lung disease. *Am. J. Respir. Cell Mol. Biol. 38*, 738−743.

(10) Koltsova, E., and Ley, K. (2009) Tyrosine sulfation of leukocyte adhesion molecules and chemokine receptors promotes atherosclerosis. *Arterioscler., Thromb., Vasc. Biol. 29*, 1709−1711.

(11) Ouyang, Y., Lane, W. S., and Moore, K. L. (1998) Tyrosylprotein sulfotransferase: purification and molecular cloning of an enzyme that catalyzes tyrosine O-sulfation, a common posttranslational modification of eukaryotic proteins. *Proc. Natl. Acad. Sci. U. S. A. 95*, 2896−2901.

(12) Beisswanger, R., Corbeil, D., Vannier, C., Thiele, C., Dohrmann, U., Kellner, R., Ashman, K., Niehr, C., and Huttner, W. B. (1998) Existence of distinct tyrosylprotein sulfotransferase genes: molecular characterization of tyrosylprotein sulfotransferase-2. *Proc. Natl. Acad. Sci. U. S. A. 95*, 11134−11139.

(13) Stone, M. J., Chuang, S., Hou, X., Shoham, M., and Zhu, J. Z. (2009) Tyrosine sulfation: an increasingly recognised post-translational modification of secreted proteins. *New Biotechnol. 25*, 299−317.

(14) Teramoto, T., Fujikawa, Y., Kawaguchi, Y., Kurogi, K., Soejima, M., Adachi, R., Nakanishi, Y., Mishiro-Sato, E., Liu, M., Sakakibara, Y., Suiko, M., Kimura, M., and Kakuta, Y. (2013) Crystal structure of human tyrosylprotein sulfotransferase-2 reveals the mechanism of protein tyrosine sulfation reaction. *Nat. Commun. 4*, 1572.

(15) Leyte, A., van Schijndel, H. B., Niehrs, C., Huttner, W. B., Verbeet, M. P., Mertens, K., and van Mourik, J. A. (1991) Sulfation of Tyr1680 of human blood coagulation factor VIII is essential for the interaction of factor VIII with von Willebrand factor. *J. Biol. Chem. 266*, 740−746.

(16) Mishiro, E., Sakakibara, Y., Liu, M. C., and Suiko, M. (2006) Differential enzymatic characteristics and tissue-specific expression of human TPST-1 and TPST-2. *J. Biochem. 140*, 731−737.

(17) Danan, L. M., Yu, Z., Ludden, P. J., Jia, W., Moore, K. L., and Learty, J. A. (2010) Catalytic mechanism of Golgi-resident human tyrosylprotein sulfotransferase-2: a mass spectrometry approach. *J. Am. Soc. Mass Spectrom. 21*, 1633−1642.

(18) Nedumpully-Govindan, P., Li, L., Alexov, E. G., Blenner, M. A., and Ding, F. (2014) Structural and energetic determinants of tyrosylprotein sulfotransferase sulfation specificity. *Bioinformatics 30*, 2302−2309.

DOI: 10.1021/acs.biochem.5b00343
Biochemistry 2015, 54, 4404−4410

(19) Siegbahn, Per E. M., and Borowski, T. (2011) Comparison of QM-only and QM/MM models for the mechanism of tyrosinase. *Faraday Discuss. 148*, 109−117.
(20) Williams, R. T., and Wang, Y. (2012) A density functional theory study on the kinetics and thermodynamics of N-glycosidic bond cleavage in 5-substituted 2′-deoxycytidines. *Biochemistry 51*, 6458−6462.
(21) Wójcik, A., Broclawik, E., Siegbahn, Per, E. M., and Borowski, T. (2012) Mechanism of benzylic hydroxylation by 4-hydroxymandelate synthase. A computational study. *Biochemistry 51*, 9570−9580.
(22) Sheng, X., and Liu, Y. (2013) Theoretical study of the catalytic mechanism of E1 subunit of pyruvate dehydrogenase multienzyme complex from *Bacillus stearothermophilus*. *Biochemistry 52*, 8079−8093.
(23) Aranda, J., Cerqueira, N. M. F. S. A., Fernandes, P. A., Roca, M., Tuñon, I., and Ramos, M. J. (2014) The catalytic mechanism of carboxylesterases: a computational study. *Biochemistry 53*, 5820−5829.
(24) Anandakrishnan, R., Aguilar, B., and Onufriev, A. V. (2012) *H++ 3.0*: automating p*K* prediction and the preparation of biomolecular structures for atomistic molecular modeling and simulations. *Nucleic Acids Res. 40*, W537−W541.
(25) Frisch, M., Trucks, G., Schlegel, H., Scuseria, G., Robb, M., Cheeseman, J., Scalmani, G., Barone, V., Mennucci, B., Petersson, G., Nakatsuji, H., Caricato, M., Li, X., Hratchian, H., Izmaylov, A., Bloino, J., Zheng, G., Sonnenberg, J., Hada, M., Ehara, M., Toyota, K., Fukuda, R., Hasegawa, J., Ishida, M., Nakajima, T., Honda, Y., Kitao, O., Nakai, H., Vreven, T., Montgomery, J., Jr., Peralta, J., Ogliaro, F., Bearpark, M., Heyd, J., Brothers, E., Kudin, K., Staroverov, V., Kobayashi, R., Normand, J., Raghavachari, K., Rendell, A., Burant, J., Iyengar, S., Tomasi, J., Cossi, M., Rega, N., Millam, J. M., Klene, M., Knox, J., Cross, J., Bakken, V., Adamo, C., Jaramillo, J., Gomperts, R., Stratmann, R., Yazyev, O., Austin, A. J., Cammi, R., Pomelli, C., Ochterski, J., Martin, R., Morokuma, K., Zakrzewski, V., Voth, G., Salvador, P., Dannenberg, J., Dapprich, S., Daniels, A., Farkas, Ö., Foresman, J., Ortiz, J., Cioslowski, J., and Fox, D. (2009) *Gaussian 09*, revision D.1, Gaussian Inc., Wallingford, CT.
(26) Zhao, Y., and Truhlar, D. G. (2008) The M06 suite of density functionals for main group thermochemistry, thermochemical kinetics, noncovalent interactions, excited states, and transition elements: two new functionals and systematic testing of four M06-class functionals and 12 other functionals. *Theor. Chem. Acc. 120*, 215−241.
(27) Calvaresi, M., Bottoni, A., and Garavelli, M. (2007) Computational clues for a new mechanism in the glycosylase activity of the human DNA repair protein hOGG1. A generalized paradigm for purine-repairing systems? *J. Phys. Chem. B 111*, 6557−6570.
(28) Calvaresi, M., Garavelli, M., and Bottoni, A. (2008) Computational evidence for the catalytic mechanism of glutaminyl cyclase. A DFT investigation. *Proteins: Struct., Funct., Genet. 73*, 527−538.
(29) Bottoni, A., Miscione, G. P., and Calvaresi, M. (2011) Computational evidence for the substrate-assisted catalytic mechanism of O-GlcNAcase. A DFT investigation. *Phys. Chem. Chem. Phys. 20*, 9568−9577.
(30) Tomasi, J., Mennucci, B., and Cammi, R. (2005) Quantum mechanical continuum solvation models. *Chem. Rev. 105*, 2999−3093.
(31) Prabhakar, R., Morokuma, K., and Musaev, D. G. (2006) Peroxynitrite reductase activity of selenoprotein glutathione peroxidase: a computational study. *Biochemistry 45*, 6967−6977.
(32) Borowski, T., and Siegbahn, P. E. M. (2006) Mechanism for catechol ring cleavage by non-heme iron intradiol dioxygenases: a hybrid DFT study. *J. Am. Chem. Soc. 128*, 12941−12953.
(33) Stenta, M., Calvaresi, M., Altoè, P., Spinelli, D., Garavelli, M., and Bottoni, A. (2008) The catalytic activity of proline racemase: a quantum mechanical/molecular mechanical study. *J. Phys. Chem. B 112*, 1057−1059.
(34) Stenta, M., Calvaresi, M., Altoè, P., Spinelli, D., Garavelli, M., Galeazzi, R., and Bottoni, A. (2009) Catalytic mechanism of diaminopimelate epimerase: a QM/MM investigation. *J. Chem. Theory Comput. 5*, 1915−1930.
(35) Calvaresi, M., Stenta, M., Garavelli, M., Altoé, P., and Bottoni, A. (2012) Computational evidence for the catalytic mechanism of human glutathione S-transferase A3−3: a QM/MM investigation. *ACS Catal. 2*, 280−286.

DOI: 10.1021/acs.biochem.5b00343
Biochemistry 2015, 54, 4404−4410